

Description of the RHIC p_{\perp} -spectra in a thermal model with expansion*

Wojciech Broniowski and Wojciech Florkowski

The H. Niewodniczański Institute of Nuclear Physics, PL-31342 Cracow, Poland

The assumption of simultaneous chemical and thermal freeze-outs of the hadron gas leads to a surprisingly accurate, albeit entirely conventional, explanation of the recently-measured RHIC p_{\perp} -spectra. The original thermal spectra are supplied with secondaries from cascade decays of all resonances, and subsequently folded with a suitably parameterized expansion involving longitudinal and transverse flow. The predictions of this thermal approach, with various parametrizations for the expansion, are in a striking quantitative agreement with the data in the whole available range of $0 \leq p_{\perp} \leq 3.5\text{GeV}$.

25.75.-q, 25.75.Dw, 25.75.Ld

In this Letter we offer a very simple explanation of the p_{\perp} -spectra recently measured at RHIC [1–3]. Our approach has the following ingredients: i) simultaneous *chemical* and *thermal* freeze-outs, with the hadron distributions given by the thermal model; in other words, hadrons decouple completely when the thermodynamic parameters reach the freezing conditions, and no particle rescattering after freeze-out is present, ii) these thermal distributions are folded with a suitably parameterized hydrodynamic expansion, involving longitudinal and transverse flow, finally, iii) feeding from resonances, including cascades, is incorporated in a complete way.

So far, the thermal approach has been applied successfully in studies of particle ratios measured in relativistic heavy-ion collisions at AGS and SPS [4–10]. Quite recently, it has also been shown that particle ratios measured at RHIC may be equally well described in the framework of such models [11–13]. Description of hadronic p_{\perp} -spectra in thermal models is more involved, since the spectra are affected by decays of resonances, hydrodynamic flow, and possibly by other phenomena occurring during the alleged phase transition from the quark-gluon plasma to a hadron gas [14]. The model results presented in this Letter are in a surprising agreement with the experiment in the entire range of the data, $0 \leq p_{\perp} \leq 3.5\text{GeV}$, as can be seen in Fig. 1. The model has two free parameters: one controlling the size of the system (overall normalization of the spectra), and the other one the transverse flow. We test two different models (parametrizations) for the freeze-out hypersurface and the hydrodynamic expansion. Both combine the Bjorken expansion [15] with transverse flow [16,17], and follow the spirit of Refs. [18–22].

The first model (model I) assumes that the freeze-out takes place at a fixed value of the invariant time, $\tau = \sqrt{t^2 - r_z^2 - r_x^2 - r_y^2} = \text{const}$, which means that, due to time dilation, the particles in the fluid elements moving farther away from the collision center decouple later than the particles in the fluid elements remaining at rest in the center-of-mass system of the colliding nuclei. Furthermore, we assume that the four-velocity of expansion

is proportional to the coordinate,

$$u^{\mu} = \frac{x^{\mu}}{\tau} = \frac{t}{\tau} \left(1, \frac{r_z}{t}, \frac{r_x}{t}, \frac{r_y}{t} \right). \quad (1)$$

The freeze-out hypersurface is parameterized as [20]

$$\begin{aligned} t &= \tau \text{ch}\alpha_{\parallel} \text{ch}\alpha_{\perp}, & r_z &= \tau \text{sh}\alpha_{\parallel} \text{ch}\alpha_{\perp}, \\ r_x &= \tau \text{sh}\alpha_{\perp} \cos\phi, & r_y &= \tau \text{sh}\alpha_{\perp} \sin\phi, \end{aligned} \quad (2)$$

where α_{\parallel} is the rapidity of the fluid element ($v_z = r_z/t = \tanh\alpha_{\parallel}$), whereas α_{\perp} describes the transverse size of the system ($\rho = \tau \text{sh}\alpha_{\perp}$). The transverse velocity is $v_{\rho} = \tanh\alpha_{\perp}/\text{ch}\alpha_{\parallel}$. We account for the finite transverse size of the system by imposing the condition $\rho = \sqrt{r_x^2 + r_y^2} < \rho_{max}$. The second model considered (model II) has the same parametrization of the four-velocity and the freeze-out hypersurface as the popular *blast* model [19,21]:

$$\begin{aligned} u^{\mu} &= (\text{ch}\alpha_{\parallel} \text{ch}\beta_{\perp}, \text{sh}\alpha_{\parallel} \text{ch}\beta_{\perp}, \cos\phi \text{sh}\beta_{\perp}, \sin\phi \text{sh}\beta_{\perp}), \\ t &= \tau \text{ch}\alpha_{\parallel}, & r_z &= \tau \text{sh}\alpha_{\parallel}, \\ r_x &= \tau \text{sh}\alpha_{\perp} \cos\phi, & r_y &= \tau \text{sh}\alpha_{\perp} \sin\phi. \end{aligned} \quad (3)$$

Both models I and II are boost-invariant. Since deviations from boost-invariance are seen in the rapidity distributions at RHIC [3], our present approach should be regarded as an approximate treatment of the mid-rapidity region. However, this approximation is very good. One may depart from the boost-invariance by limiting the integration in the α_{\parallel} variable, thus limiting the longitudinal size of the system. The results for the spectra obtained that way are very similar to the boost-invariant results presented below even for the limit for α_{\parallel} as low as 0.5.

The local freeze-out conditions, *i.e.*, the values of the temperature and the chemical potentials, are universal for the whole freeze-out hypersurface. Since for boost-invariant models the particle ratios at mid-rapidity are not affected by the expansion (this important point is discussed below), the values of the thermodynamic parameters may be obtained directly from the standard thermal analysis, which yields [13] $T = 165 \pm 7\text{MeV}$,

$\mu_B = 41 \pm 5\text{MeV}$, $\mu_S = 9\text{MeV}$, and $\mu_I = -1\text{MeV}$. Knowing T and μ 's we calculate the local distribution functions of hadrons which include the *initial thermal contribution*, as well as additional contributions from the *sequential two- and three-body decays of all heavier resonances*. These decays are very important, since they *effectively cool* the system by 35-40 MeV, as recently shown in Ref. [13], and also known from earlier works on other reactions [23,24]. The standard Cooper-Frye-Schonberg formula [25] is used to calculate the p_\perp -spectra of the observed hadrons. As the result, the particle densities are obtained as the integrals over the freeze-out hypersurface, $N_i = \int d^3p/p^0 \int p^\mu d\Sigma_\mu f_i(p \cdot u)$, where $d\Sigma_\mu$ is the volume element of the hypersurface, f_i is the phase-space distribution function for particle species i (composed from the initial and secondary particles), and $p^\mu = (m_\perp \text{ch} y, m_\perp \text{sh} y, p_\perp \cos \varphi, p_\perp \sin \varphi)$ is the four-momentum. Finally, we find, for the case of model I, the rapidity and transverse-momentum distributions of hadrons,

$$\frac{dN_i}{d^2p_\perp dy} = \tau^3 \int_{-\infty}^{+\infty} d\alpha_\parallel \int_0^{\rho_{\max}/\tau} \text{sh}\alpha_\perp d(\text{sh}\alpha_\perp) \times \int_0^{2\pi} d\xi p \cdot u f_i(p \cdot u), \quad (4)$$

where $p \cdot u = m_\perp \text{ch}(y - \alpha_\parallel) \text{ch}\alpha_\perp - p_\perp \cos \xi \text{sh}\alpha_\perp$ and $\xi = \phi - \varphi$. Similarly, for model II the relevant parameters are the velocity, β_\perp , and the volume of the system [19,21]. We observe that the rapidity distribution (4) is boost-invariant, since the dependence on y can be absorbed in the integration variable by shifting $\alpha_\parallel \rightarrow \alpha_\parallel + y$. Clearly, this is a direct consequence of the assumed boost-invariant form of the freeze-out surface.

In the thermal-model fit of particle ratios of Ref. [13] one computes the integrals $N_i = V \int d^3p f_i(\sqrt{m_i^2 + p^2})$. The question arises whether the ratios obtained that way, which correspond to the collection of particles from the whole phase space, are the same as the ratios experimentally measured in the mid-rapidity region, *i.e.*, the ratios of the integrals $dN_i/dy = \int d^2p_\perp dN_i/(d^2p_\perp dy)$. The answer is yes, and follows from the boost-invariance of the expansion model. Indeed, since dN_i/dy are independent of y , we have

$$\frac{dN_i/dy}{dN_j/dy} = \frac{\int dy dN_i/dy}{\int dy dN_j/dy} = \frac{N_i}{N_j}. \quad (5)$$

This obvious general result can be verified explicitly in our specific boost-invariant models.

Figure 1 shows our main result. In Fig. 1 (a,b) we compare the model predictions for the p_\perp -spectra of pions, kaons, protons and antiprotons, with the PHENIX *minimum bias* preliminary data [1]. The model parameters are fitted by the χ^2 method including all points in the range $0 < p_\perp < 2\text{GeV}$ from Fig. 1 (a,b). This

yields $\tau = 5.55\text{fm}$, $\rho_{\max} = 4.50\text{fm}$ for model I, and $\mathcal{V} = (6.48\text{fm})^3$, $\beta_\perp = 0.52$ for model II. The statistical errors in the fitted parameters are of the order of 1%. In Fig. 1 (c) we compare the model predictions to preliminary PHENIX [1] and STAR [2] data for the *most central* collisions. The model parameters are fitted by the least-square method to all points in Fig. 1 (c), yielding $\tau = 7.66\text{fm}$, $\rho_{\max} = 6.69\text{fm}$ for model I, and $\mathcal{V} = (9.81\text{fm})^3$, $\beta_\perp = 0.52$ for model II. It is natural that the size parameters of the system for the most central collisions are larger than for the minimum-bias case, which averages over centralities. The size parameters correspond to the size of the system, in particular for central collisions in model I $\rho_{\max} = 6.69\text{fm}$ is very close to the radius of the Au nucleus, 6.22fm. We note that the quality of the fit in Fig. 1 is impressive. For the minimum-bias data (Fig. 1 (a,b)) model I (thicker lines) crosses virtually all data points within error bars, with $\chi^2/\text{degree of freedom}$ less than 1. Amusingly, also the very-high p_\perp data are reproduced. The fit with model II is very similar in the range $0 < p_\perp < 2\text{GeV}$, and falls slightly below the data at higher p_\perp , where hard processes are expected to contribute. The fit to the most central collisions, Fig 1 (c), is of similar quality except for the \bar{p} preliminary data from STAR, which fall 30-50% below the model fits at low p_\perp . Note, however, that at low p_\perp the STAR and PHENIX preliminary data are not fully consistent. The total multiplicity of charged particles produced in the most central event measured at PHOBOS [27], $555 \pm 12 \pm 35$, is consistent with size parameters quoted above, and yields $\tau \simeq 7\text{fm}$ for model I and $\mathcal{V} \simeq (9\text{fm})^3$ for model II.

Since the values of the strange and isospin chemical potentials are very close to zero, the model predictions for π^+ and π^- , as well as for K^+ and K^- are practically the same. The value of the baryon chemical potential of 41 MeV splits the p and \bar{p} spectra. Note the convex shape of the pion spectra in Fig. 1, reproduced by the model. In addition, the π^+ and p curves in Fig. 1 cross at $p_\perp \simeq 2\text{GeV}$, and the K^+ and p at $p_\perp \simeq 1\text{GeV}$, exactly as in the experiment. We stress that our method is different from traditional fits in the blast or similar models, where the temperatures for various particles are being adjusted independently or from semi-empirical formulas. We have no freedom here: the temperature is the freeze-out temperature fixed by the particle ratios, and the spectra are obtained as described in Ref. [13].

In Table 1 we present the inverse slope parameters, T_{eff} , defined by fitting the function $\text{const exp}(-m_\perp/T_{\text{eff}})$ to the data *, and average p_\perp . Agreement of model I and the data for the inverse slopes is within error bars

* Note that this definition depends on the fitting region in m_\perp . Thus, the resulting numbers depend quite strongly on

except for most central \bar{p} data from PHENIX (2.5 standard deviations) and K^- and \bar{p} data from STAR (2 and 4.6 standard deviations, respectively). The values of $\langle p_\perp \rangle$ are within error bars.

We end this Letter with a more pedagogical discussion of the role of various effects included in our analysis. In Fig. 2 the dotted line shows the initial pion p_\perp -spectrum in a static fireball with the same temperature and chemical potentials as used in our calculation. No secondaries are included here. The effect of the decays of *all* resonances is represented by the dashed-dotted line, representing the sum of the initial and secondary pions. Decays of the resonances lead to an *effective decrease of the temperature* by about 35-40 MeV [13], since the emitted particles tend to populate the low- p_\perp region. However, the spectrum remains concave. The effect of the pure longitudinal Bjorken expansion (with $\tau = \sqrt{t^2 - r_z^2} = \text{const}$) is illustrated by the dashed line. This is a *redshift* effect, since all fluid elements move away from the observer, which leads to extra cooling of the spectrum. The solid line corresponds to model I (model II gives very similar results), incorporating both the longitudinal expansion and the transverse flow. The transverse flow causes some fluid element to move in the direction of the observer, leading to *blueshift* [28]. Hence we find a combination of redshift and blueshift, yielding the p_\perp spectrum displayed by the solid line in Fig. 3. Note that the spectrum finally acquires the convex shape, as seen in the experiment (*cf.* Fig. 1). The effects of blueshift are stronger for more massive particles, hence the behavior of Fig. 1 and Table 1.

To conclude, we emphasize that the presented description, implementing in a simple fashion all key ingredients: freeze-out, decays of resonances, and longitudinal and transverse flows, works for RHIC in the whole available range of data. We stress that we have assumed that the chemical and thermal freeze-outs occur simultaneously, which is in the spirit of the sudden hadronization of Refs. [29,30]. A practical value of our results is that they give hints and constraints for more involved hydrodynamic calculations, *e.g.* [31–33], by providing the freeze-out conditions that describe the data. A natural extensions of the model should include different centrality effects (elliptic flow), and rapidity dependence. Also, the model must be further verified against the available data from the HBT pion interferometry [34]. Note that our size parameters are very similar to the experimental HBT radii. We have checked that our model works also for the SPS

this region, and T_{eff} is a largely-biased measure of the particle spectra. Following Ref. [1], we use $0.3\text{GeV} < p_\perp < 0.9\text{GeV}$ for the pions, $0.55\text{GeV} < p_\perp < 1.6\text{GeV}$ for K^+ , p , and \bar{p} , and $0.75\text{GeV} < p_\perp < 1.6\text{GeV}$ for K^- . The χ^2 fits are performed in these regions.

The details of these studies will be presented elsewhere.

We are grateful to Ulrich Heinz for extensive and useful discussions.

* Supported in part by the Polish State Committee for Scientific Research, grant 2 P03B 09419.

- [1] J. Velkovska for the PHENIX Collaboration, nucl-ex/0105012; A. Bazilevsky for the PHENIX Collaboration, nucl-ex/0105017.
- [2] J. W. Harris for the STAR Collaboration, in [3].
- [3] Proceedings of the *Quark Matter 2001* conference, BNL, January 2001, Nucl. Phys. A (in print).
- [4] P. Braun-Munzinger, J. Stachel, J. P. Wessels, and N. Xu, Phys. Lett. B **344**, 43 (1995); Phys. Lett. B **365**, 1 (1996).
- [5] J. Rafelski, J. Letessier, and A. Tounsi, Acta Phys. Pol. B **28**, 2841 (1997).
- [6] J. Cleymans, D. Elliott, H. Satz, and R. L. Thews, Z. Phys. C **74**, 319 (1997).
- [7] P. Braun-Munzinger, I. Heppe, and J. Stachel, Phys. Lett. B **465**, 15 (1999).
- [8] G. D. Yen and M. I. Gorenstein, Phys. Rev. C **59**, 2788 (1999).
- [9] F. Becattini, J. Cleymans, A. Keranen, E. Suhonen, and K. Redlich, Phys. Rev. C **64**, 024901 (2001).
- [10] M. Gaździcki, Nucl. Phys. A **681**, 153 (2001).
- [11] J. Rafelski, J. Letessier, and G. Torrieri, Phys. Rev. C **64**, 054907 (2001).
- [12] P. Braun-Munzinger, D. Magestro, K. Redlich, and J. Stachel, hep-ph/0105229.
- [13] W. Florkowski, W. Broniowski, and M. Michalec, nucl-th/0106009.
- [14] J. Dolejší, W. Florkowski, and J. Hüfner, Phys. Lett. B **349**, 18 (1995).
- [15] J. D. Bjorken, Phys. Rev. D **27**, 140 (1983).
- [16] G. Baym, B. Friman, J.-P. Blaizot, M. Soyeur, and W. Czyż, Nucl. Phys. A **407**, 541 (1983).
- [17] P. Milyutin and N. N. Nikolaev, Heavy Ion Phys **8**, 333 (1998); V. Fortov, P. Milyutin, and N. N. Nikolaev, JETP Lett. **68**, 191 (1998).
- [18] P. J. Siemens and J. Rasmussen, Phys. Rev. Lett. **42**, 880 (1979); P. J. Siemens and J. I. Kapusta, Phys. Rev. Lett. **43**, 1486 (1979).
- [19] E. Schnedermann, J. Sollfrank, and U. Heinz, Phys. Rev. C **48**, 2462 (1993).
- [20] T. Csörgő and B. Lörstad, Phys. Rev. C **54**, 1390 (1996).
- [21] D. H. Rischke and M. Gyulassy, Nucl. Phys. A **697**, 701 (1996); Nucl. Phys. A **608**, 479 (1996).
- [22] R. Scheibl and U. Heinz, Phys. Rev. C **59**, 1585 (1999).
- [23] J. Sollfrank, P. Koch, and U. Heinz, Phys. Lett. B **252**, 256 (1990).
- [24] G. E. Brown, J. Stachel, and G. M. Welke, Phys. Lett. B **253**, 19 (1991).
- [25] F. Cooper, G. Frye, and E. Schonberg, Phys. Rev. D **11**,

- 192 (1975).
- [26] J. Cleymans, H. Oeschler, and K. Redlich, *J. Phys. G* **25**, 281 (1999).
 - [27] B. B. Back *et al.*, PHOBOS Collaboration, *Phys. Rev. Lett.* **85**, 3100 (2000).
 - [28] U. Heinz, *Nucl. Phys. A* **661**, 140 (1999).
 - [29] J. Rafelski and J. Letessier, *Phys. Rev. Lett.* **85**, 4695 (2000).
 - [30] G. Torrieri and J. Rafelski, *New Jour. Phys.* **3**, 12 (2001).
 - [31] D. Teaney, J. Lauret, and E. V. Shuryak, *Phys. Rev. Lett.* **86**, 4783 (2001); nucl-th/0104041, in [3].
 - [32] P. Huovinen, P. F. Kolb, U. Heinz, P. V. Ruuskanen, and S. A. Voloshin, *Phys. Lett. B* **503**, 58 (2001).
 - [33] P. Huovinen, nucl-th/0108033.
 - [34] C. Adler *et al.*, STAR Collaboration, *Phys. Rev. Lett.* **87**, 082301 (2001).

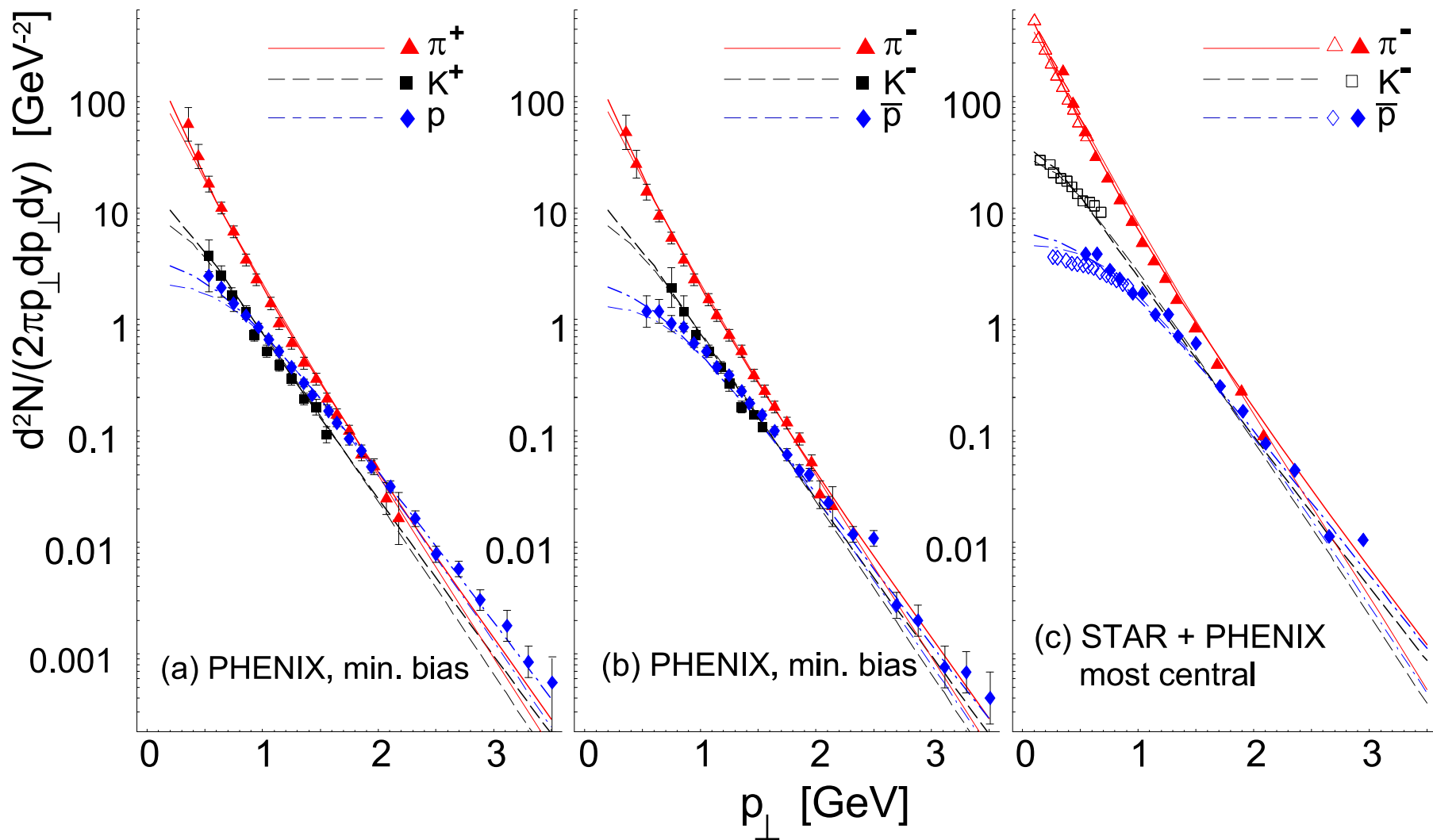


FIG. 1. The p_{\perp} -spectra at $y = 0$ of pions (solid line), kaons (dashed line) and protons or antiprotons (dashed-dotted line), as evaluated from model I (thicker lines) and model II (thinner lines), compared to the PHENIX preliminary minimum-bias data (a,b), and to STAR (open symbols) and PHENIX preliminary highest-centrality data (c) ($Au + Au$ at 130GeV).

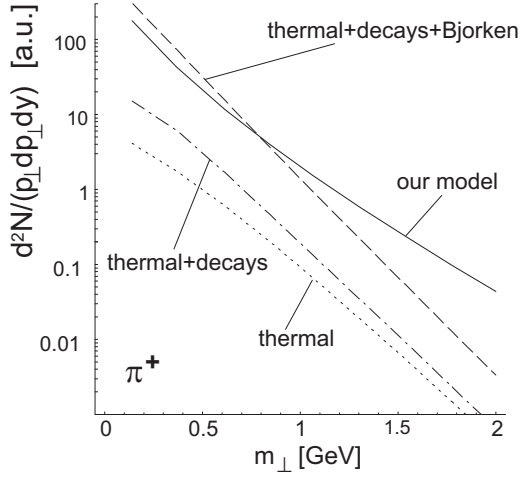


FIG. 2. Contributions of various effects to the p_{\perp} -spectra of π^+ (normalizations arbitrary).

TABLE I. Inverse slope parameters, T_{eff} , and the average transverse momentum, $\langle p_{\perp} \rangle$.

T_{eff} [MeV]	π	K	p or \bar{p}
PHENIX, min. bias, exp.	190 ± 17	272 ± 16	274 ± 11
positive hadrons model I	203	263	292
PHENIX, min. bias, exp.	207 ± 20	260 ± 17	301 ± 14
negative hadrons model I	202	255	291
PHENIX, most central, exp.	197 ± 19	-	367 ± 23
negative hadrons model I	206	273	310
STAR, most central, exp.	188 ± 20	300 ± 35	560 ± 50
negative hadrons model I	176	223	327
$\langle p_{\perp} \rangle$ [MeV]	π	K	p or \bar{p}
PHENIX, most central, exp.	370 ± 70	600 ± 60	840 ± 50
positive hadrons model I	438	629	853
PHENIX, most central, exp.	370 ± 70	630 ± 80	860 ± 50
negative hadrons model I	434	629	852